Electronic Interactions and Photoinduced Electron Transfer in Covalently Linked Porphyrin−C_{60}(pyridine) Diads and Supramolecular Triads Formed by Self-Assembling the Diads and Zinc Porphyrin

Francis D'Souza,*,† Gollapalli R. Deviprasad,† Melvin E. Zandler,† Mohamed E. El-Khouly,‡ Mamoru Fujitsuka,‡ and Osamu Ito*,‡

Department of Chemistry, Wichita State University, 1845 Fairmount, Wichita, Kansas 67260-0051, and Institute of Multidisciplinary Research for Advanced Materials, Tohoku University, Katahira, Sendai, 980-8577, Japan

Received: February 14, 2002

Supramolecular triads of the type (donor-1)−acceptor:(donor-2) composed of free-base porphyrin, fullerene, and zinc porphyrin, have been formed by a "covalent-coordinate" approach. Toward this, two diads, namely, 5-(3′-(2″-(3‴ or 4‴-pyridyl)fulleropyrrolidinyl-*N*)ethoxyphenyl)-10,15,20-triphenylporphyrin, bearing C_{60} as acceptor and free-base porphyrin, H_2P, as donor were first synthesized. The diads and self-assembled supramolecular triads, which were formed by coordinating the pyridine group located on the diads to zinc tetraphenylporphyrin, ZnP, have been characterized by semiempirical PM3, electrochemistry, and steady-state and time-revolved spectroscopic techniques. Subpicosecond and nanosecond transient absorption spectral studies of diads revealed the occurrence of the electron transfer from the H_2P moiety to the C_{60} entity via the excited singlet state of H_2P. Clear evidence for the formation of triads in *o*-dichlorobenzene was obtained from the steady-state and time-resolved fluorescence measurements, which revealed quenching of the ZnP emission on addition of the pyridine bearing diads. Semiempirical PM3 energy optimized structures of the triads suggested substantial intramolecular interactions between the H_2P and C_{60} entities. Cyclic voltammetric studies on these triads exhibited a total of 12 one-electron redox processes involving the three redox active ZnP, H_2P, and C_{60} entities. Nanosecond transient absorption studies revealed additional charge separation in the triads as compared to that observed for the diads, suggesting that the coordinated ZnP accelerates the charge-separation process. However, in a coordinating solvent such as benzonitrile, intermolecular electron transfer from the ^{3}ZnP* to the diads is shown to take place.

Introduction

Studies of supramolecular systems bearing redox and photoactive entities are valuable for designing light energy harvesting systems as well as for developing redox and optoelectronic devices.[1,2] Covalent attachment of donor−acceptor entities with one or more spacer units to control the distance and orientation has been the popular choice[2] even though noncovalent linkage is considered nature's choice of assembling the different redox and photoactive entities in the active centers of biological systems.[3] In this regard, a few elegantly designed self-assembled donor−acceptor type diads and supramolecular systems bearing one or more different type of the chromophores have been synthesized and studied.[2] These diads contain electron donor chromophore such as porphyrins, phthalocyanines, or ruthenium(II) tris(bipyridine) and electron acceptors of the type quinone, nitroaromatic compounds, metal complexes, pyrromellitic anhydride, etc.[1−4] Recently, fullerenes[5] have drawn special attention as electron acceptors owing to their three-dimensional structure,[6] reduction potentials comparable to benzoquinone,[7] absorption spectrum extending over most of the visible spectral region[8] and a small re-organization energy in electron-transfer reactions.[9] Several covalently linked donor−acceptor systems[10−12] and a few self-assembled via metal−ligand coordination donor−acceptor systems[13,14] bearing fullerene have been reported.

In the present study, we have utilized a "covalent-coordinate" bonding approach to form supramolecular triads consisting of covalently linked free-base porphyrin−C_{60} diads, i.e., 5-(3′-(2″-(3‴ or 4‴-pyridyl)fulleropyrrolidinyl-*N*)ethoxyphenyl)-10,15,-20-triphenylporphyrin (compounds **1** and **2** in Scheme 1) and (tetraphenylporphyrinato)zinc (ZnP). In the diads, the fulleropyrrolidine is functionalized to bear a pyridyl moiety that is subsequently utilized to coordinate ZnP to obtain the desired supramolecular triads composed of free-base porphyrin (H_2P), C_{60}, and ZnP entities (**3** and **4** in Scheme 1). That is, (donor-1)−acceptor:(donor-2) type triads, in which the (donor-1)−acceptor refers to the covalently linked entities and the acceptor:(donor-2) refers to the entities held by a coordinate bond. The electrochemical behavior of the redox active diads and supramolecular triads has been investigated. Efficient intramolecular electron transfer from the singlet excited free-base porphyrin to the covalently attached fullerene has been observed in the studied diads in *o*-dichlorobenzene and benzonitrile. Interestingly, upon coordination of the pyridine entity of **1** or **2** to ZnP to form the supramolecular triads, one would expect a competition between electron-transfer from the singlet excited ZnP and/or H_2P to C_{60} and/or energy-transfer from the singlet excited ZnP to H_2P. The present investigations show that the second donor, ZnP of the triads actually accelerates the charge-separation process and the energy-transfer quenching involving excited ZnP and H_2P is not an efficient process.

† Wichita State University.
‡ Tohoku University.

10.1021/jp0204307 CCC: $22.00 © 2002 American Chemical Society
Published on Web 04/18/2002

SCHEME 1

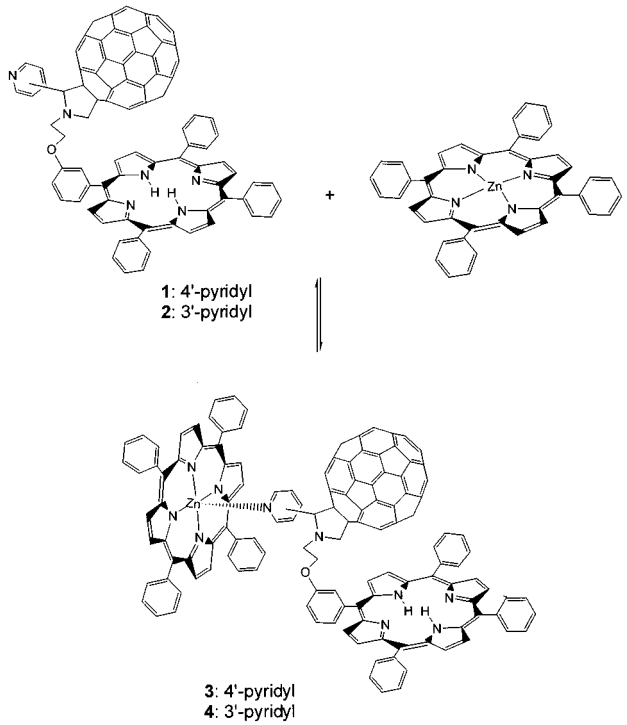

Experimental Section

Chemicals. Buckminsterfullerene, C_{60} (+99.95%) was either from BuckyUSA (Bellaire, TX) or SES Research (Houston, TX). Benzonitrile and *o*-dichlorobenzene in sure seal bottles were from Aldrich Chemicals (Milwaukee, WI), and tetra-*n*-butylammonium perchlorate, (TBA)ClO_4, was from Fluka Chemicals. Solvents used in the present study are all purest grade commercially available. The synthesis of free-base porphyrin covalently linked to 2-pyridylfulleropyrrolidine (**1** and **2**) is described elsewhere.[14] All the compounds were freshly purified by column chromatography, and their purity was tested by TLC prior to spectral measurements.

Instrumentation. The UV−visible spectral measurements were carried out with a Shimadzu Model 1600 UV−visible spectrophotometer. The fluorescence was monitored by using a Spex Fluorolog spectrometer. A right angle detection method was used. Cyclic voltammograms were obtained by using a conventional three electrode system on an EG&G Model 263A potentiostat/galvanostat. A platinum disk electrode was used as the working electrode. A platinum wire served as the counter electrode. An Ag/AgCl electrode, separated from the test solution by a fritted supporting electrolyte/solvent bridge, was used as the reference electrode. The potentials were referenced to an internal ferrocene/ferrocenium redox couple. All the solutions were purged prior to the spectral and electrochemical measurements using argon gas.

Computational Calculations. The PM3 semiempirical energy minimization calculations of the diads and triads were carried out by using *GAUSSIAN 98*.[15] The compounds were optimized to a stationary point on the Born-Oppenheimer potential energy surface.

Time-Resolved Emission and Transient Absorption Measurements. Nanosecond transient absorption spectra in the NIR region were measured by means of laser-flash photolysis; 532 nm light from a Nd:YAG laser was used as the exciting source and a Ge-avalanche-photodiode module was used for detecting the monitoring light from a pulsed Xe-lamp, as described in our previous reports.[16] The picosecond time-resolved fluorescence spectra were measured using an argon-ion pumped Ti:sapphire laser (Tsunami) and a streak scope (Hamamatsu Photonics). The details of the experimental setup are described elsewhere.[16] The subpicosecond transient absorption spectra were recorded by the pump and probe method. The samples were excited with a second harmonic generation (SHG, 388 nm) of output from a femtosecond Ti:sapphire regenerative amplifier seeded by SHG of a Er-dropped fiber (Clark-MXRCPA-2001 plus, 1 kHz, fwhm 150 fs). The excitation light was depolarized. The monitor white light was generated by focusing the fundamental laser light on a flowing D_2O/H_2O cell. The transmitted monitor light was detected with a dual MOS linear image sensor (Hamamatsu Photonics, C6140) or InGaAs photodiode array (Hamamatsu Photonics, C5890-128).

Results and Discussion

The optical absorption spectra of the diads **1** and **2** revealed bands corresponding to the free-base porphyrin and fulleropyrrolidine entities.[14] The absorption maxima of the free-base porphyrin entity showed a small red shift (1−2 nm) compared to the spectrum of pristine *meso*-tetraphenylporphyrin, H_2P, suggesting the occurrence of weak $\pi-\pi$ type ground-state interactions between the free-base porphyrin and C_{60} entities in the diads. Concentration dependence studies (10−200 μM) revealed no changes in the absorption maxima, suggesting that the interactions are mainly intramolecular in nature. These observations suggest that the covalently linked fulleropyrrolidine with flexible bonds intramolecularly interacts with the porphyrin π-system in solution. In the case of triads formed by treating **1** or **2** with ZnP (1:1), a red shift of the ZnP Soret band was observed, indicating the formation of a pentacoordinated ZnP.[17] However, on increasing addition of **1** or **2** to the solution of ZnP, such spectral shifts were masked due to the strong absorption of H_2P entity of **1** or **2** in the wavelength region.

Further, to envision the structure of the diads and triads, energy minimization calculations using semiempirical PM3 methods were performed on the flexibly linked free-base porphyrin-C_{60} diads and self-assembled free-base porphyrin−C_{60}:zinc porphyrin triads. Figure 1 shows the structures obtained (at local minima) for **1** at two extreme conformations. That is, a "folded" conformer in which the free-base porphyrin and the fulleropyrrolidine are close enough to have through space interactions and, an "extended" conformer, in which the two entities are further apart. It may be mentioned here that owing to the presence of flexible bonds several intermediate structures are possible, representing several local minima. In the "folded" conformer, the center-to-center distance between the free-base porphyrin and C_{60} spheroid was estimated to be 8.8 Å while the edge-to-edge distance was 5.2 Å. In the "extended" conformer, the center-to-center distance between H_2P and C_{60} was found to be 14.4 Å while the edge-to-edge distance was 7.5 Å. The enthalpy of formation for the "folded" conformer was found to be 1088.1 kcal mol^{-1}, while this value for the "extended" conformer was 1083.4 kcal mol^{-1}. That is, the "extended" conformer is 4.7 kcal more stable than the "folded" conformer in a noninteracting environment (gas phase).

The energy minimized structures of the triads, **3** and **4**, obtained by self-assembling **1** or **2** and ZnP are shown in Figure 2. For triad **3**, the two porphyrin rings were aligned in a L-shape with an angle of 100° between the two porphyrin rings (Figure 2a). The *meso*-C of ZnP is found to be in the plane of H_2P ring atoms. The C_{60} entity was located over the H_2P ring similar to that shown in Figure 1a. The angle between the C_{60} center, H_2P

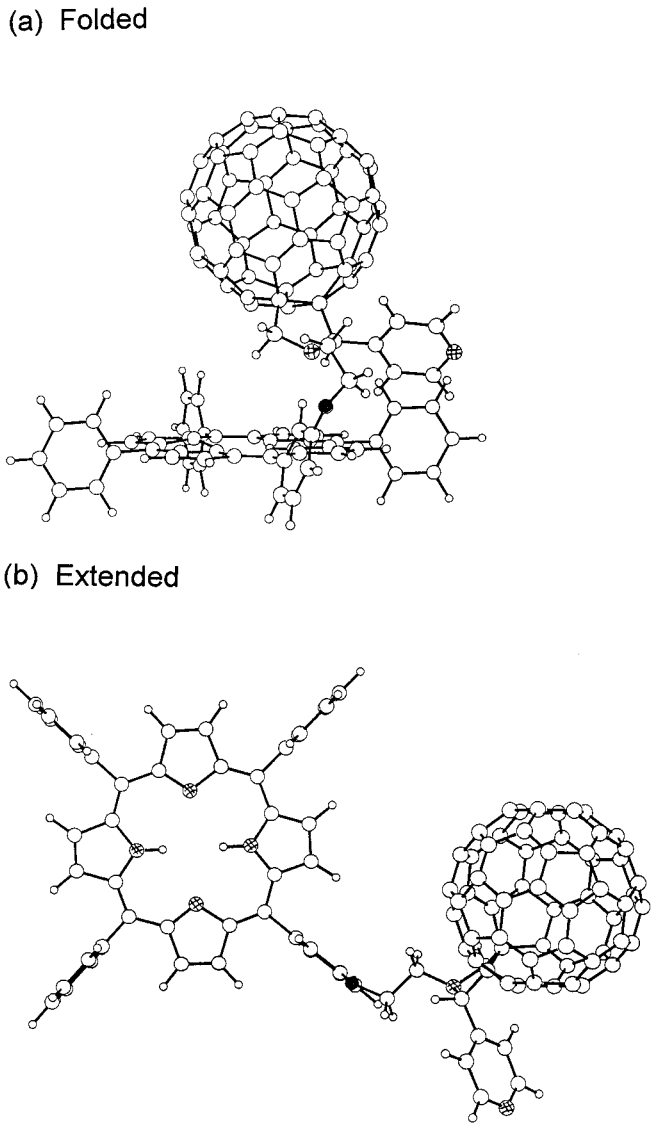

Figure 1. Semiempirical PM3 energy minimized structure of **1** in (a) "folded" and (b) "extended" forms: filled circle, oxygen; hatched circle, nitrogen.

center, and ZnP center was found to be 49°. The estimated center-to-center distance between C_{60} and ZnP moieties was found to be 10.2 Å, while this distance between C_{60} and H_2P and between ZnP and H_2P were found to be 8.7 and 10.6 Å, respectively. The estimated edge-to-edge distance between ZnP-(α-C) and C_{60} was found to be 6.4 Å, while these distances between H_2P(N) and C_{60} and ZnP(*meso*-C) and H_2P(β-C) were found to be 5.1 and 5.7 Å, respectively.

For triad **4**, the two porphyrin rings were aligned in a V-shape with an angle of 75° between the two porphyrin rings. Like in **3**, the C_{60} entity of **4** was also found to be located over the H_2P ring (Figure 2b). The angle between the C_{60} center, H_2P center, and ZnP center was found to be 62°. The estimated center-to-center distance between C_{60} and ZnP moieties was found to be 8.3 Å, while this distance between C_{60} and H_2P and between ZnP and H_2P were found to be 9.2 and 12.5 Å, respectively. The estimated edge-to-edge distance between ZnP(β-C) and C_{60} was found to be 4.5 Å, while these distances between H_2P(N) and C_{60} and ZnP(*meso*-C) and H_2P(β-C) were found to be 6.8 and 8.4 Å, respectively. These results collectively suggest the existence of closely spaced to one another entities of the triads with substantial intramolecular interactions between the H_2P and

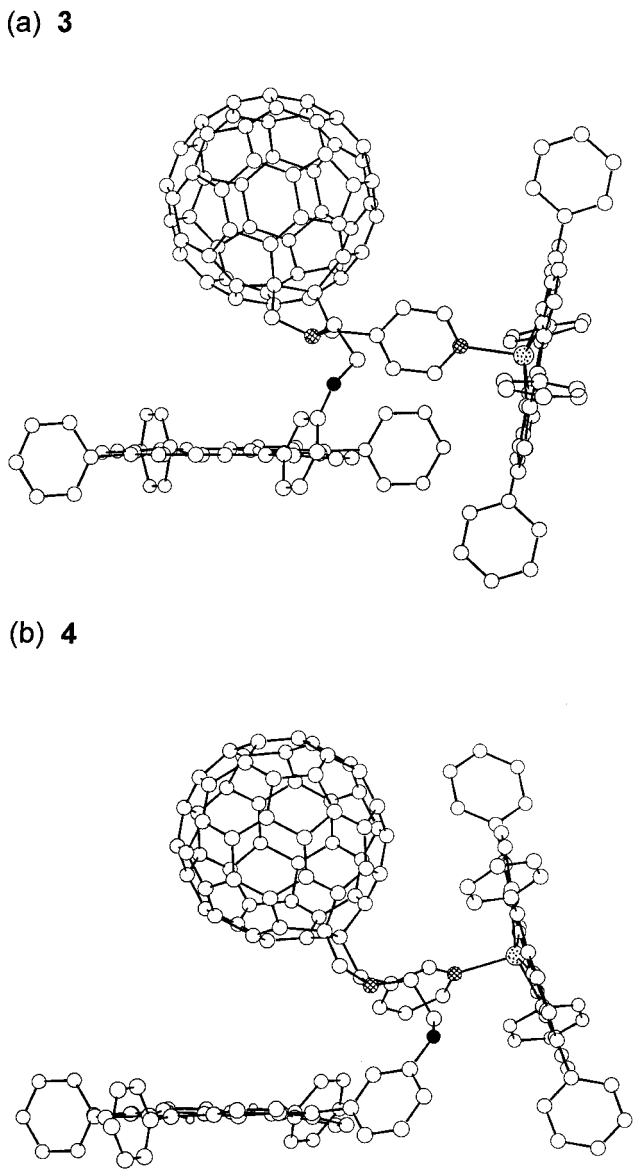

Figure 2. Semiempirical PM3 energy minimized structure of (a) triad **3** and (b) triad **4**: filled circle, oxygen; hatched circle, nitrogen; dotted circle, zinc.

C_{60} entities. The difference in the enthalpy of formation, ΔH_f, between the self-assembled triads and the sum of the heats of formation of the diads and ZnP was found to be 7.8 kcal mol^{-1} for **3** and 5.7 kcal mol^{-1} for **4**, respectively. These values compare with a value of 5.8 kcal mol^{-1} obtained for the 2-(pyrid-4-yl)fulleropyrrolidine axially coordinated to ZnP by PM3 methods.

Electrochemistry. The rich electrochemistry of porphyrins[18] and fullerenes[7,19] has in recent years attracted wide attention owing to their potential applications in building redox switches, molecular electronic devices, electrocatalysts, mimicking biological active sites etc.[2e−f,4,11n] Tuning of the redox potentials of fullerenes was often achieved by functionalization of the fullerene bearing either electron donor or electron acceptor entities or by varying fullerene size.[19] In the case of porphyrins, in addition to the functionalization of porphyrins bearing peripheral substituents, redox tuning was also achieved by a selection of different metal ions in the porphyrin cavity.[18] Determination of the redox potential in the newly developed molecular donor−acceptor type systems is important to evaluate the energetic of electron-transfer reactions.[4] With this in mind,

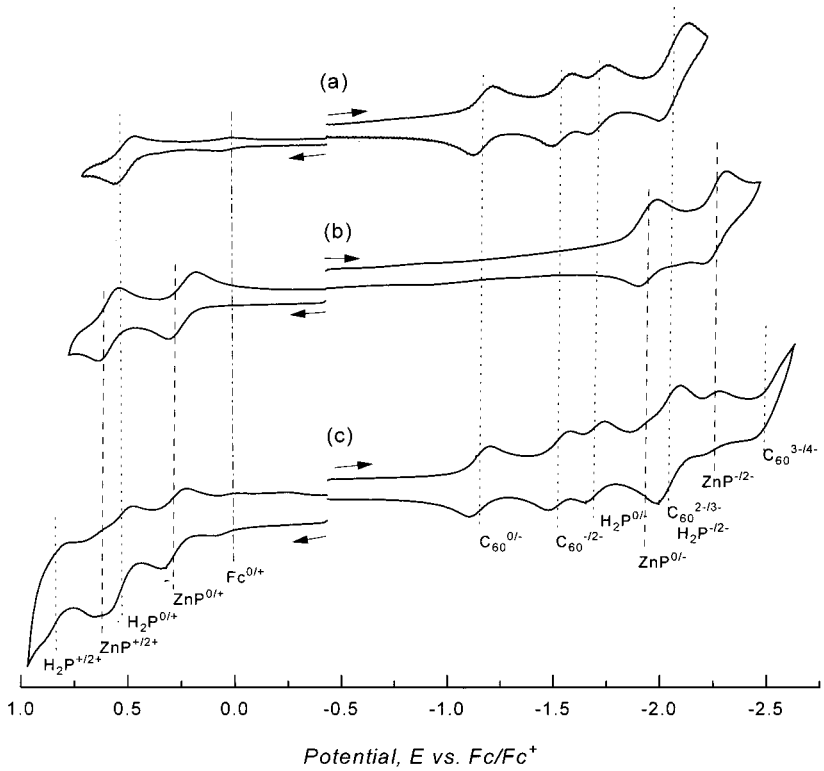

Figure 3. Cyclic voltammograms of (a) diad **1** and (b) ZnP and (c) supramolecular triad **3** in 0.1 M (TBA)ClO_4, *o*-dichlorobenzene. Scan rate = 100 mV/s. Note the overlapping third reduction of C_{60} and second reduction of free-base porphyrin. The $Fc^{0/+}$ represents the ferrocene/ferrocenium redox couple used as an internal standard.

TABLE 1: Electrochemical Half-Wave Redox Potentials (V vs Fc/Fc^+) of the Porphyrin−C_{60}(pyridine) Diads and the Supramolecular Porphyrin−C_{60}(pyridine):Zinc Porphyrin Triads in *o*-Dichlorobenzene, 0.1 M (TBA)ClO_4

	potential *E*, V vs. Fc/Fc^+											
compound	$H_2P^{+/2+}$	$ZnP^{+/2+}$	$H_2P^{0/+}$	$ZnP^{0/+}$	$C_{60}^{0/-}$	$C_{60}^{-/2-}$	$H_2P^{0/-}$	$ZnP^{0/-}$	$C_{60}^{2-/3-}$	$H_2P^{-/2-}$	$ZnP^{-/2-}$	$C_{60}^{3-/4-}$
H_2P	0.79[a]		0.53				−1.75			−2.05		
ZnP		0.62		0.28				−1.92			−2.23	
C_{60}(pyridine)[b]					−1.10	−1.49			−1.95			−2.44[a]
1	0.80[a]		0.55		−1.14	−1.51	−1.68		−2.04[c]	2.04[c]		−2.45[a]
2	0.82[a]		0.56		−1.14	−1.52	−1.68		−2.05[c]	−2.05[c]		−2.46[a]
3[d]	0.81[a]	0.64	0.57	0.30	−1.10	−1.44	−1.65	−1.90	−2.00[b]	−2.00[b]	−2.20	−2.47[a]
4[d]	0.83[a]	0.65	0.58	0.29	−1.11	−1.45	−1.67	−1.93	−2.01[b]	−2.01[b]	−2.01	−2.47[a]

[a] Quasireversible. [b] From ref 13a. [c] Two one-electron process due to the overlap of the second reduction of free-base porphyrin and the third reduction of fulleropyrrolidine entities. [d] Obtained by slow precipitation of the diads **1** or **2** with equimolar amounts of ZnP.

we have performed a systematic study to evaluate the redox behavior of the diads and the supramolecular triads using cyclic voltammetric technique.

Figure 3a shows representative cyclic voltammograms of the diad **1** in 0.1 M (TBA)ClO_4, *o*-dichlorobenzene. Within the accessible potential window of the solvent, up to 8 one-electron redox processes were observed for the diads (only the six reversible redox processes are shown in the figure). The redox potential corresponding to the first oxidation of the free-base porphyrin of **1** was located at $E_{1/2} = 0.55$ V, while the second quasireversible process was located at $E_{1/2} = 0.80$ V vs Fc/Fc^+. The reduction potentials of the appended fulleropyrrolidine entity of **1** were located at $E_{1/2} = -1.14$, -1.51, -2.04, and -2.45 V vs Fc/Fc^+. The first redox potential corresponding to the free-base porphyrin reduction was located at -1.68 V, while the second redox process overlaps with the third reduction process of fulleropyrrolidine. An almost similar electrochemical behavior was observed for **2** (Table 1). A comparison between the redox potentials of the diads with that of the free-base porphyrin, H_2P, and 2-pyridylfulleropyrrolidine,[13a] recorded under similar solution conditions revealed small anodic shifts of 10−40 mV, suggesting the existence of ground-state interactions between the porphyrin π-ring and the C_{60} spheroid.

The cyclic voltammogram of ZnP utilized to form the supramolecular triads via axial coordination of the appended pyridyl group of fulleropyrrolidines is shown in Figure 3b. The redox potentials corresponding to the oxidation were located at 0.28 and 0.62 V vs Fc/Fc^+, while the potentials corresponding to the reduction were located at -1.92 and -2.23 V vs Fc/Fc^+, respectively.

The cyclic voltammogram of supramolecular triad **3** obtained by slow precipitation of the diad in the presence of ZnP is shown in Figure 3c. A total of 12 one-electron processes that include four one-electron oxidations corresponding to the oxidations of the two porphyrin rings, and eight one-electron reductions corresponding to the reductions of the two porphyrin rings and one fullerene entity were observed within the accessible potential window of the solvent. Similar electrochemical behavior was also observed for the supramolecular triad **4**. The site of electron transfer for each of the redox process was deduced from control experiments involving fulleropyrrolidine, ZnP, H_2P, diads, and titrations involving the diads and zinc porphyrin. Table 1 lists

SCHEME 2

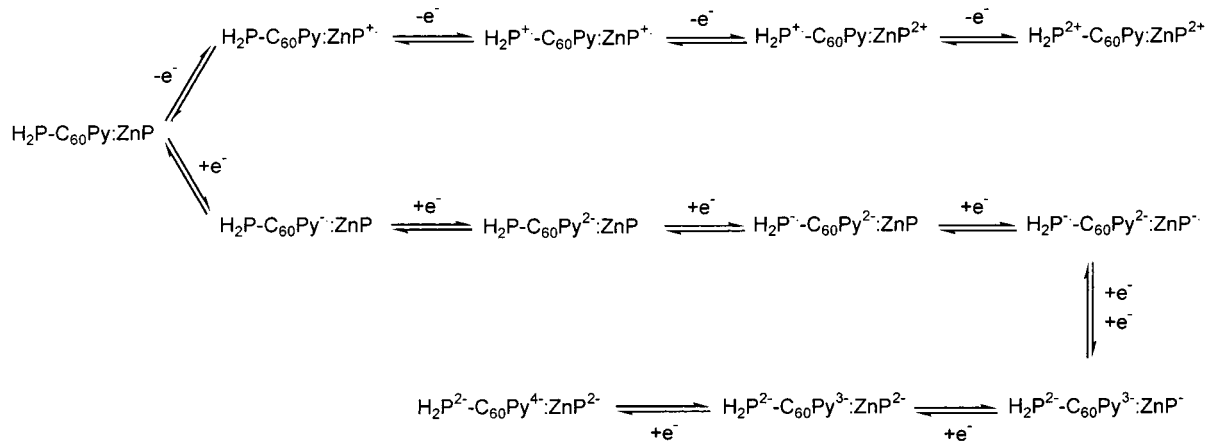

the redox potentials corresponding to the oxidation and reduction of the different entities while Scheme 2 illustrates the occurrence of the site of electron transfer during each redox process.

In the supramolecular triads, the potentials for the zinc porphyrin oxidations were shifted anodically by 10−20 mV as compared to the potentials of pristine ZnP in the absence of an axial ligand, and this could be a consequence of the formation of pentacoordinated zinc complex or weak electronic interactions between the zinc porphyrin π-ring and C_{60} spheroid. A similar anodic shift of 20−40 mV was also observed for the fullerene redox potentials as compared to the corresponding redox potentials of the diads. Though these shifts are smaller in magnitude, this trend is clearly observed. These results collectively suggest the existence of weak interactions between the different entities of the supramolecular triads. The easier oxidation of zinc porphyrin compared to the free-base porphyrin suggests that the zinc porphyrin is a better electron donor in the investigated triads. Importantly, the one-electron redox processes corresponding to the three different redox entities established the molecular integrity of the triad.

Steady-State Fluorescence Emission Studies. The steady-state emission spectra of the diads, **1** and **2**, revealed two emission bands located at 665 and 720 nm, respectively. The intensity of these bands was significantly quenched as compared to *meso*-tetraphenylporphyrin owing to the presence of the appended C_{60}. The observed fluorescence quantum yields (Φ_f) of the H_2P moiety in **1** and **2** were found to be 0.0077 and 0.0072, respectively, which was smaller than that of H_2P ($\Phi_f = 0.13$).[20] The picosecond time-resolved emission studies, and the subpicosecond and nanosecond transient absorption spectral studies revealed that this quenching is mainly due to the occurrence of electron transfer from the singlet excited state of the H_2P moiety to the C_{60} moiety (vide infra).

Figure 4 shows the changes of the fluorescence emission spectra of ZnP on addition of increasing amounts of **1** in *o*-dichlorobenzene. In the absence of added diads, ZnP exhibits two emission bands at 598 and 646 nm.[21] The intensity of the 598 nm emission of ZnP decreased on addition of **1** with the appearance of two new emission bands located at 665 and 720 nm corresponding to the H_2P emission.[21] The observed decrease of ZnP emission confirms interaction between **1** and ZnP, thus suggesting the formation of a supramolecular triad.[22] For the reasons of the observed decrease of ZnP emission, the occurrence of one or both of the following processes is suggested: (i) electron-transfer quenching from the excited singlet state of ZnP to the fullerene entity and (ii) excited energy transfer from ZnP to the fullerene entity or to the bound via axial ligation

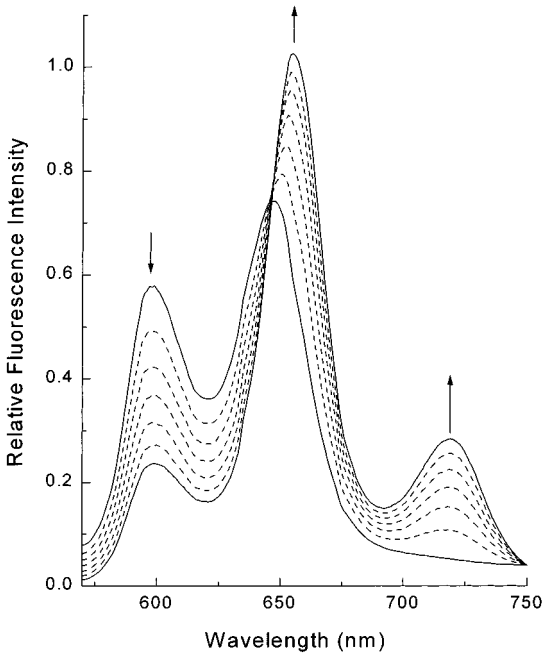

Figure 4. Uncorrected steady-state fluorescence spectrum of ZnP on increasing addition of **1** to form the triad **3** in *o*-dichlorobenzene. Concentration of ZnP employed is 20 μM and each addition of **1** is equivalent to 20 μM until 6 equiv was reached; $\lambda_{ex} = 550$ nm.

free-base porphyrin within the supramolecular entity. In the following sections the time-resolved emission spectral results are discussed in order to verify the different quenching pathways.

Picosecond Time-Resolved Fluorescence Studies. The fluorescence time profiles of **1** and H_2P in *o*-dichlorobenzene are shown in Figure 5. The time profile of H_2P exhibited a monoexponential decay with a lifetime, τ_f, of 13.5 ns, and this compares with the literature value of 13.6 ns. The fluorescence time profiles of the diads, **1** and **2**, could be fitted satisfactorily to a biexponential decay. The lifetimes of the short component are found to be about 440 ps (38%) for **1** and 710 ps (63%) for **2**, suggesting the occurrence of intramolecular electron-transfer from the singlet excited H_2P to the fullerene entity in **1**. Changing the solvent to a relatively more polar benzonitrile revealed slightly different lifetime values. That is, the lifetimes of the short components were found to be around 430 (63%) and 410 ps (66%), respectively, for **1** and **2**. The lower values of the lifetimes compared to that observed in *o*-dichlorobenzene could be ascribed to enhanced electron-transfer quenching in

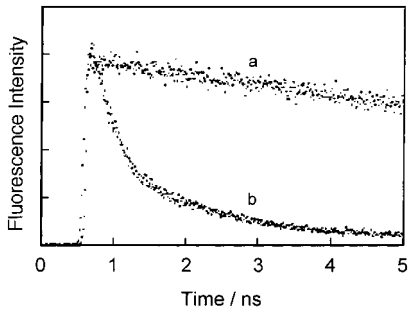

Figure 5. Fluorescence decay profiles of (a) H_2P (~20 μM) and (b) **1** (~20 μM) at 720 nm in *o*-dichlorobenzene; λ_{ex} = 410 nm. Initial intensities are normalized.

TABLE 2: Fluorescence Lifetimes (τ_f), Charge-Separation Rate Constants (k_{cs}),[a] Charge-Separation Quantum Yields (Φ_{cs})[b] of the Covalently Linked Diads and Supramolecular Triads in *o*-Dichlorobenzene (DCB) and Benzonitrile (BN)

compound	solvent	λ_{em}, nm	τ_f/ns (%)		k_{cs}/s^{-1}	Φ_{cs}
ZnP[c]	DCB	600	2.10 (100)			
1[c]	DCB	720	0.44 (38)	1.46 (62)	2.2×10^9	0.97
1[c]	BN	720	0.43 (63)	1.96 (37)	2.2×10^9	0.97
1+ ZnP (6:1)[c]	DCB	600	1.78 (100)		8.5×10^7	(0.03)[d]
		720	0.47 (40)	1.49 (60)	2.1×10^9	0.97
1+ ZnP (1:1)[c]	DCB	600	1.99 (100)		2.6×10^7	(0.01)[d]
		720	0.50 (42)	1.54 (58)	2.0×10^9	0.96
2[d]	DCB	720	0.71 (63)	1.92 (37)	1.3×10^9	0.95
2[d]	BN	720	0.41 (66)	1.42 (34)	2.4×10^9	0.97
2 + ZnP (6:1)[c]	DCB	600	1.83 (100)		1.0×10^8	(0.05)[d]
		720	0.71 (60)	1.84 (40)	1.3×10^9	0.95
2 + ZnP (1:1)[c,e]	DCB	600	1.99 (100)		2.6×10^7	(0.02)[d]
		720	0.75 (52)	1.92 (48)	1.2×10^9	0.93

[a] $k_{cs} = (1/\tau_f)_{sample} - (1/\tau_f)_{ref}$, in which short lifetime was employed for τ_f for biexponential decay. The τ_f value = 13.6 ns was employed for H_2P. [b] $\Phi_{cs} = [(1/\tau_f)_{sample} - (1/\tau_f)_{ref}]/(1/\tau_f)_{sample}$. [c] Concentration of porphyrin used = 0.04 mM; λ_{ex} = 410 nm. [d] Φ_{cs} in parentheses is calculated as ratio of the calculated k_{cs}. [e] The estimated k_{cr} for the present diads and triads is approximately 5.0×10^7 s^{-1}.

more polar benzonitrile. The evaluated fluorescence lifetimes (τ_f) are summarized in Table 2, in which the charge-separated rates (k_{cs}) and quantum yields (Φ_{cs}), evaluated in an usually manner from the shorter τ_f values assuming that all the quenching was due to the charge separation from the singlet excited state of H_2P.[23] The data in Table 2 indicate fast and high efficiency of charge separation in the investigated diads. A comparison of the charge-separation rates between **1** and **2** in moderately polar *o*-dichlorobenzene suggested that the rate and efficiency for **1** are relatively higher than that for **2**, and this has been ascribed to the presence of different solution configurations.

For the biexponential decay of the diads, a frequently observed spectral feature for the charge-separation process in donor−acceptor type diads, the slower decay has been attributed to a delayed fluorescence process produced by the charge-recombination of the radical ion pairs.[9,10] In the present study, we have not further attempted to elucidate the slower fluorescence decay path of the biexponential decay of the diads.

The results of time-resolved fluorescence spectra of **1** or **2** in the presence of different amounts of added ZnP are also listed in Table 2. The lifetimes at two emission wavelengths, i.e., at 600 nm corresponding to ZnP emission and 720 nm corresponding to H_2P emission were monitored. In the absence of ZnP, no emission at 600 nm was observed. Interestingly, in agreement with steady-state fluorescence results, addition of 6 equiv of **1** or **2** to a solution of ZnP in *o*-dichlorobenzene, that is, an experimental condition in which majority of the ZnP in solution is bound to the diads **1** or **2** to form the triads **3** or **4**, revealed slight acceleration of quenching of the ZnP emission at 600 nm; for **1**:ZnP (6:1 equiv), the lifetime of ZnP is found to be 1.78 ns and for **2**:ZnP (6:1 equiv) the corresponding lifetime of ZnP was 1.83.

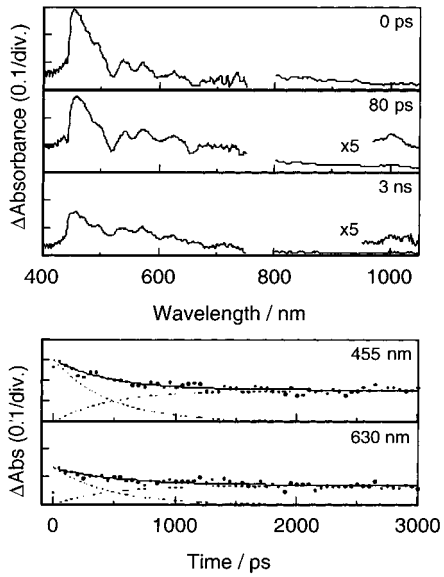

Figure 6. Picosecond transient absorption spectra obtained by the 388 nm laser photolysis for **1** (~20 μM) and the time profiles for the transient peaks at 455 and 630 nm in benzonitrile; dotted lines in the time profiles are curve-resolved lines.

On addition of ZnP (1 equiv) to a solution of **1** or **2**, the τ_f value of ZnP in *o*-dichlorobenzene (1.99 ns) became closer to that of uncoordinated ZnP (2.10 ns). Also, the emission monitored at 720 nm corresponding to the H_2P emission did not reveal any significant changes in the lifetime, suggesting that the energy-transfer quenching is an unlikely process. Further addition of ZnP increased the uncoordinated ZnP, thus returning τ_f of ZnP to 2.10 ns monitored at 600 nm. In benzonitrile, the τ_f value did not reveal any appreciable changes on addition of either **1** or **2**, suggesting absence of coordination between the pyridyl entity of **1** or **2** to ZnP.

The rates of charge transfer from the singlet excited ZnP in the supramolecular triads were calculated from the difference in the lifetimes of the free ZnP, as listed in Table 2. The quantum yields for the charge-separation process via the excited singlet state of ZnP in the supramolecular triads were calculated by the ratio of the charge-separation rate via the ZnP to that via the H_2P of the diads. Small but appreciable contribution of the charge separation via ZnP to the total charge separation was observed in the supramolecular triads in *o*-dichlorobenzene (Table 2).

Picosecond Transient Absorption Spectral Studies. To prove the charge separation in the subpicosecond time region as revealed by the fluorescence studies, we have performed the picosecond transient absorption measurements of **1** and **2**. Figure 6 shows the time-resolved spectra of **1** in benzonitrile; the spectrum obtained immediately after the 150 fs laser pulse (spectrum at 0 ps in Figure 6) has been attributed to the singlet−singlet transitions of both H_2P and fulleropyrrolidine moieties.[24,25] After 80 ps of the laser pulse, the absorption bands in the region of 550 to 650 nm became broad and the 1000 nm band was clear, in which the former can be ascribed to the cation radical of the H_2P moiety and the latter to the anion radical of the fulleropyrrolidine moiety. After 3 ns, the bands in the region 550−650 nm became rather flat accompanied by a decreased intensity of the 1000 nm band. Similar transient spectra were

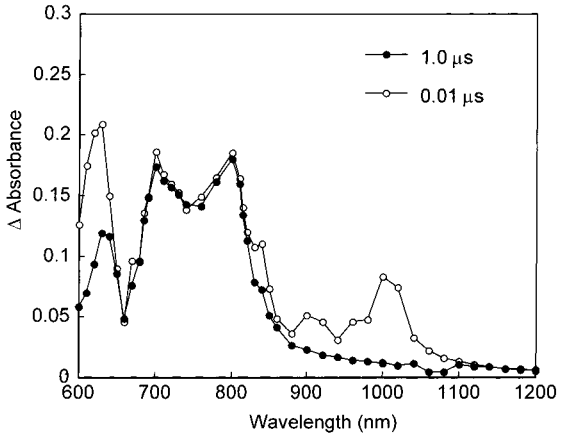

Figure 7. Transient absorption spectra obtained by the 532 nm laser photolysis of **1** in *o*-dichlorobenzene; cross in vacant circle is spectrum at 0.01 μs and filled circle at 1 μs.

observed in *o*-dichlorobenzene. For **2**, almost similar spectral changes were observed in both solvents. The time profiles were curve-resolved, as shown in dotted lines. The k_{cs} values evaluated from the initial parts of the decays of the singlet−singlet transition of H_2P and rises of the radical-cation absorptions at 455 and 630 nm were found to be 2.2×10^9 s^{-1} for **1** and 2.6×10^9 s^{-1} for **2**, which are in good agreement with those evaluated from fluorescence lifetimes. The k_{cr} value evaluated from the decay in the later part than 2000 ps, is found to be about $(2-3) \times 10^7$ s^{-1} for **1** and **2**. It may be mentioned here that in the case of the triad, the laser pulse and monitoring light changed the color of ZnP in the chlorinated solvent, *o*-dichlorobenzene; hence, clear picosecond transient absorption spectra could not be obtained.

Nanosecond Transient Absorption Spectral Studies. The nanosecond transient absorption spectrum of pristine ZnP exhibited absorption peaks at 630 and 840 nm corresponding to the triplet state.[24,25] Similarly, pristine H_2P exhibited transient absorption bands at 620 and 800 nm corresponding to its triplet state.[24,25] The transient absorption spectrum of 2-(pyrid-4-yl)-fulleropyrrolidine revealed a band around 700 nm corresponding to its triplet state.[24] The anion radical of 2-(pyrid-4-yl)-fulleropyrrolidine is expected to reveal a band around 1000 nm, while the cation radicals of H_2P and ZnP are expected to appear at 620 nm.

The nanosecond transient absorption spectrum of **1** showed a peak around 1000 nm in addition to the 700 nm band of the triplet C_{60}, and 620 and 800 nm bands corresponding to the triplet state of the free-base porphyrin (Figure 7).[25] The 1000 nm band has been attributed to the radical anion of the C_{60} moiety, which only appeared in the spectrum at 0.01 μs, indicating that the anion radical of the C_{60} moiety appears and decays quickly (see Figure 8 for the time profiles). A part of the transient absorption band at 626 nm also showed quick decay and this has been attributed to the formation of $H_2P^{\bullet+}$. In the case of **2**, the transient absorption spectra also showed the 1000 nm band in addition to the triplet states of C_{60} and H_2P.

Figure 8 shows the time profiles in the absence and presence of oxygen for the various peaks of **1** in the transient spectrum. The absorption intensities of the triplet states (at 700 and 800 nm and the slow decay parts at 630 and 1000 nm) were all long-lived in the absence of oxygen, while they decayed in the presence of oxygen in about 500 ns. For the 1000 nm peak, the quick rise−decay component was not affected in the presence of oxygen, while the slow-decay part was almost completely

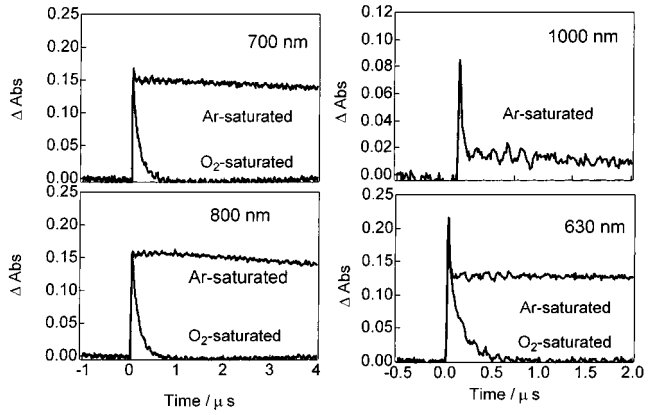

Figure 8. Time profiles for the 700, 800, 1000, and 630 nm transient peaks in the presence and absence of oxygen observed for **1** in Figure 7 in *o*-dichlorobenzene.

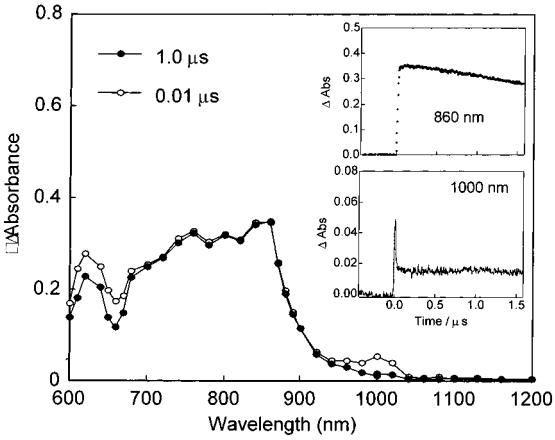

Figure 9. Transient absorption spectra obtained by the 532 nm laser photolysis of ZnTPP and **1** (1:1) in *o*-dichlorobenzene; cross in open circle at 0.01 μs and filled circle is spectrum at 1 μs. Inset: time profiles at 860 and 1000 nm in the presence and absence of oxygen.

quenched by oxygen, which indicated that the slow-decay part at 1000 nm is the absorption tail of $^3H_2P^*$.

The above observations of the quick rise−decay band at 625 and 1000 nm clearly indicate the formation of the ion pair via intramolecular charge separation from the singlet excited H_2P to the C_{60} moiety, which is in good agreement with the short fluorescence lifetime of H_2P and the picosecond transient absorption spectra. The rate constant evaluated from the quick decay (ca. $(3-4) \times 10^7$ s^{-1}) may be attributed to the charge-recombination process of the radical ion-pair state.

The relative efficiency of intramolecular charge separation has been evaluated by monitoring the absorbance ratio of the 1000 nm band to that of the 700 nm band (A_{1000nm}/A_{700nm}). In the nanosecond transient spectra at 0.01 μs, the absorbance ratio was found to be 0.45 for **1** and 0.32 for **2**, respectively. Two routes have been considered for the formation of the triplet states. The first route involves the charge recombination of the radical ion pair yielding the triplet state[25] and the second one involves the intersystem crossing from the excited singlet state of H_2P and C_{60} moieties. However, it has not been possible to evaluate their relative contributions since the laser duration and power employed in the nanosecond transient absorption measurements are quite different from that employed for the fluorescence-lifetime measurements using picosecond laser.

As shown in Figure 9, the transient absorption spectrum of **1** revealed the existence of the 1000 nm band on addition of equimolar amounts of ZnP, although the intensity was lower

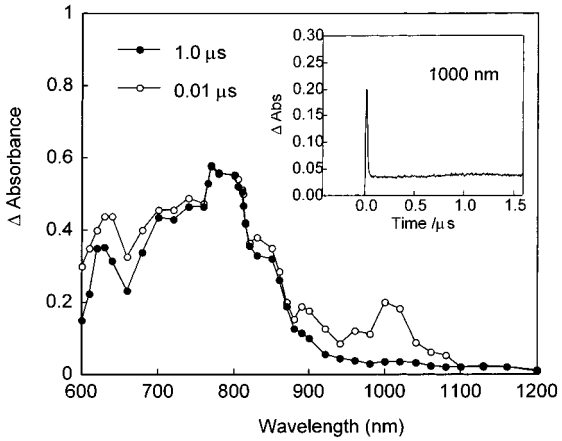

Figure 10. Transient absorption spectra obtained by the 532 nm laser photolysis of **1** and ZnP (6:1) in *o*-dichlorobenzene; cross in open circle at 0.01 μs and filled circle is spectrum at 1 μs. Inset: time profile at 1000 nm.

compared with other transient bands due to the triplet states. A new band at 850 nm corresponding to the triplet state of ZnP was also observed. The intensity of this band was higher than that of the corresponding H_2P band, indicating the formation of more excited ZnP than the H_2P moiety in **1**. Thus, the A_{1000nm}/A_{700nm} value (0.24) is smaller than the ratio of 0.45 observed for **1** in the absence of ZnP, because electron-transfer efficiency from ^{1}ZnP* to the C_{60} moiety connected by a coordinate bond is lower than the ^1H_2P* covalently linked C_{60} moiety. Similar spectral trends have been observed for **2** in the presence of ZnP; that is, the A_{1000nm}/A_{700nm} value is found to be 0.14, which is relatively smaller than a value of 0.32 observed for **2** in the absence of ZnP. On further addition of ZnP to the solution of **1** or **2** (6:1 equiv) in *o*-dichlorobenzene, excess free ZnP hindered the observation of accelerated charge-separation in the supramolecular triads.

Interestingly, on addition of 6 equiv of **1** or **2** to a solution of ZnP to form the triads **3** and **4** with no appreciable amounts of free ZnP left in solution,[22] the 1000 nm band revealed an increased intensity (Figure 10) as compared to those shown in Figures 7 and 9. For triads **3** and **4**, the estimated A_{1000nm}/A_{700nm} values were found to be 0.50 and 0.52, respectively, which are higher than those observed for **1** and **2** in the absence of any ZnP (0.45 and 0.32) and in the presence of equimolar ZnP (0.24 and 0.14). These results clearly suggest accelerated charge separation in the triads compared to the corresponding diads where the axially coordinated ZnP acts as an electron donor to the fulleropyrrolidine entity.

In benzonitrile, a noncoordinating solvent, quite different transient spectra and time profiles were observed. As shown in Figure 11, a slow rise of the 1000 and 620 nm were observed in addition to quick rise and decay due to intramolecular charge separation. The slow rises at 1000 and 620 nm are accompanied by the appreciable decays at 750 and 850 nm, which suggests that intermolecular second-order electron transfer takes place via the triplet excited states of ZnP and **1** (or **2**). From the rise rates of the ion radicals and decay rates of the triplet state of ZnP, the second-order rate constants (k_{et}^{inter}) for the intermolecular electron-transfer process were evaluated to be 1.4×10^8 and 1.9×10^8 $M^{-1}s^{-1}$ for **1** and **2**, respectively, on assuming a unit quantum yield for the intermolecular electron-transfer process from the triplet state of free ZnP to the C_{60} moieties in **1** and **2**. These values are about an order or magnitude smaller than that reported for electron-transfer process from ^{3}ZnP* to

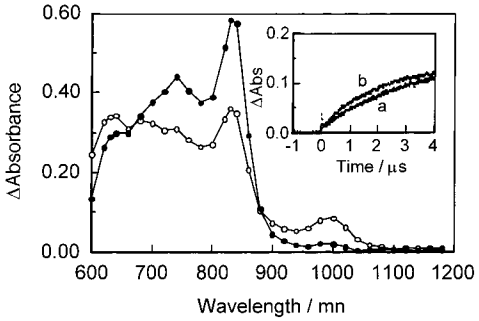

Figure 11. Transient absorption spectra obtained by the 532 nm laser photolysis of **1** in the presence of ZnP (1:1) in benzonitrile; open circle is spectrum at 0.25 μs and filled circle is spectrum at 2.5 μs. Inset: time profiles at 1000 nm (a) ZnP:**1** = 1:1 equiv and (b) 6:1 equiv.

pristine C_{60} in benzonitrile.[26] The decreased rates have been attributed to the associated steric effects of the H_2P moiety in **1** and **2**.

In *o*-dichlorobenzene, appreciable decays of the absorption bands 750 and 850 nm were not observed (Figure 10);[27] furthermore, appreciable rise of 1000 nm band was not observed after the quick decay, as shown in the inserted time profile in Figure 10. These results suggest the absence of intermolecular electron transfer in *o*-dichlorobenzene and provide further evidence for the coordination of ZnP to the pyridine moiety in **1** and **2** forming supramolecular triads. In *o*-dichlorobenzene, the fast charge separation via the singlet states of H_2P moieties and coordinated ZnP follows a quick charge recombination within the supramolecular triads.

Figure 12 illustrates energy level diagrams summarizing the observed photochemical events in the diads and triads in *o*-dichlorobenzene. For the diads, the quenching pathway is mainly through electron transfer from the singlet excited free-base porphyrin to the covalently linked C_{60} entity in *o*-dichlorobenzene and benzonitrile. The charge recombination of radical ion pair, $H_2P^{\bullet+}-C_{60}Py^{\bullet-}$ may further produce the $^3C_{60}$-Py* and ^3H_2P* in addition to the direct production of the ground states of the diads. Energetically, the possibility of regenerating ^1H_2P* and $^1C_{60}Py$* by charge recombination of $H_2P^{\bullet+}-C_{60}Py^{\bullet-}$ is found to be low. It may be mentioned here that the efficiencies for the charge-separation processes in **1** and **2** in benzonitrile are as high as that reported for a rigidly linked (phenylamide) diad involving H_2P and C_{60} entities, although the charge-separation rates are slightly smaller.[28] One reason for this may be the intramolecular interactions that could facilitate the charge separation, as shown in Figure 1a.

As depicted in Figure 12b for the supramolecular (donor-1)−acceptor:(donor-2) type triads, energy transfer from ^{1}ZnP* to $H_2P-C_{60}Py$ is possible; however, in the absence of a rise of the fluorescence at 720 nm corresponding to H_2P emission, such an energy-transfer process is unlikely to occur. For the radical ion-pair formation via the charge separation in the supramolecular triads, two kinds of the radical ion-pair products can be envisioned. First, formation of the radical ion-pair product from the singlet excited free-base porphyrin, $H_2P^{\bullet+}-C_{60}Py^{\bullet-}$:ZnP and second, formation of the radical ion-pair product from the singlet excited zinc porphyrin or fullerene, $H_2P-C_{60}Py^{\bullet-}$:$ZnP^{\bullet+}$. The present fluorescence-lifetime studies demonstrate that the former is the main quenching pathway, while the latter is a minor one. The measured efficiency of charge separation is found to be relatively higher for the triads as compared to the diads, suggesting the coordinated ZnP accelerates the charge-separation process acting as an electron donor in *o*-dichlorobenzene.

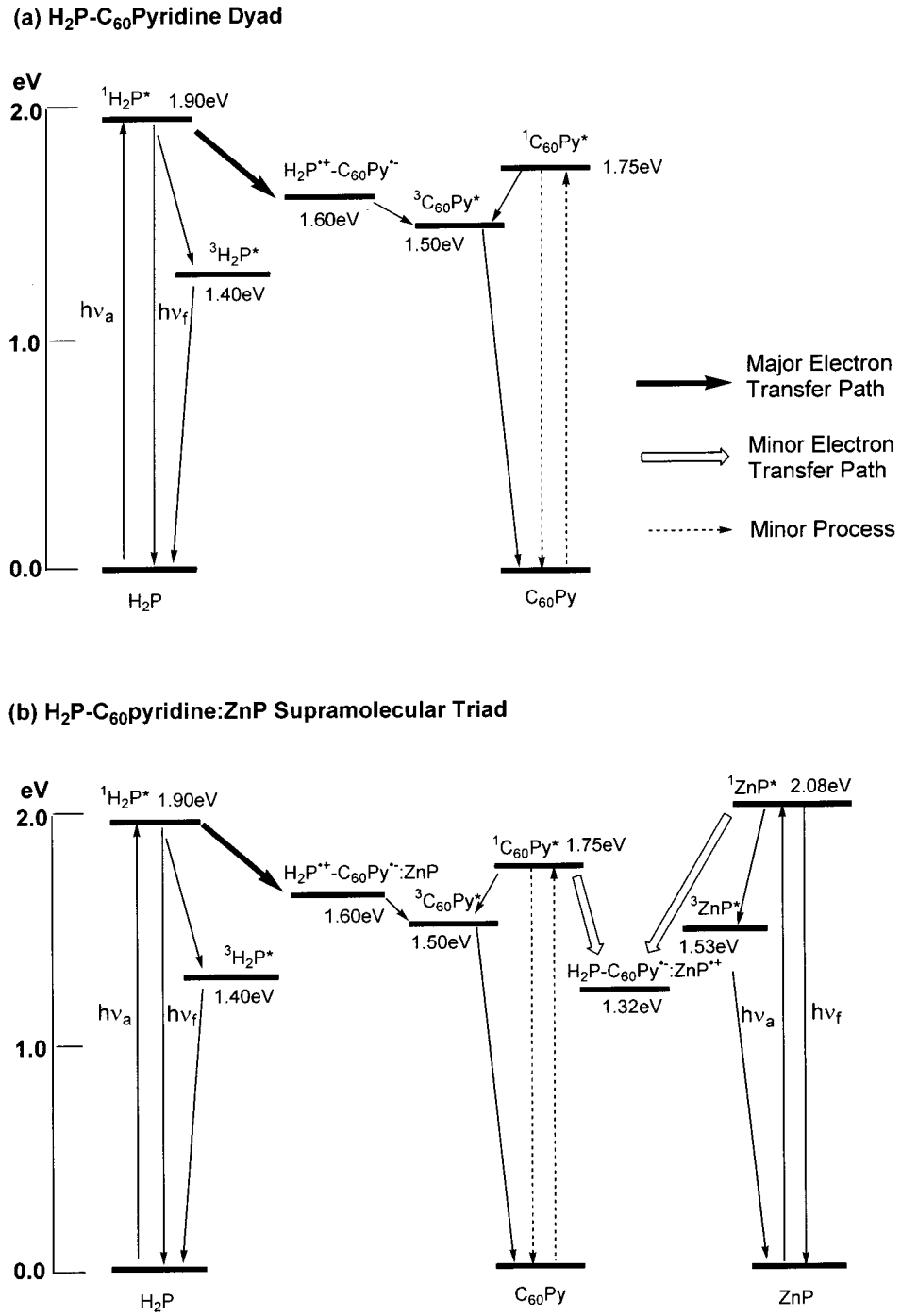

Figure 12. Energy level diagrams showing the different photochemical events for (a) free-base porphyrin linked C_{60}(pyridine) diad, $H_2P-C_{60}Py$, and (b) supramolecular free-base porphyrin linked C_{60}(pyridine):zinc porphyrin, $H_2P-C_{60}Py$:ZnP, triads in *o*-dichlorobenzene.

Summary

We have demonstrated the formation of supramolecular triads by the presently developed covalent-coordinate approach.

The covalently linked by flexible bonds diads, 5-(3′-(2″-(3‴ or 4‴-pyridyl)fulleropyrrolidinyl-*N*)ethoxyphenyl)-10,15,20-triphenylporphyrin, revealed weak intramolecular type interactions between the free-base porphyrin ring and C_{60} spheroid in the ground states. Semiempirical calculations performed by PM3 methods also suggested the existence of such intramolecular interactions. Cyclic voltammetric studies revealed up to eight one-electron reversible redox processes for each of the diads within the potential window of *o*-dichlorobenzene containing 0.1 M (TBA)ClO_4. The observed efficient quenching of the free-base porphyrin fluorescence has been attributed to the occurrence of electron transfer from the singlet excited free-base porphyrin to the covalently linked C_{60} by subpicosecond and nanosecond transient absorption spectral studies combined with the fluorescence-lifetime measurements.

By utilizing the pyridine group located on the fulleropyrrolidine entity of the diads, self-assembled supramolecular triads were formed by coordinating the pyridine moiety to the zinc tetraphenylporphyrin. The PM3 energy optimized structure of the triads suggested the existence of closely spaced to one another entities of the triads with substantial intramolecular interactions between the H_2P and the C_{60} entities. Cyclic voltammetric studies revealed a total of 12 one-electron redox

reactions involving all the three redox active, free-base porphyrin, zinc porphyrin, and C_{60} entities within the potential window of *o*-dichlorobenzene containing 0.1 M $(TBA)ClO_4$. The steady-state fluorescence studies revealed quenching of zinc porphyrin emission. The fluorescence lifetimes monitored at both the zinc porphyrin and free-base porphyrin emission peak positions revealed slight quenching of the zinc porphyrin, in addition to the quenching of free-base porphyrin. Nanosecond transient absorption studies revealed additional charge separation in the triads as compared to that observed for the diads, suggesting that the second donor, ZnP, in the triads accelerates the charge-separation process in *o*-dichlorobenzene. In benzonitrile, on the other hand, an intermolecular second-order electron transfer takes place from the triplet states of ZnP to the C_{60} entity of the diads. The absence of such intermolecular second-order electron-transfer reactions in *o*-dichlorobenzene is important evidence of the formation of supramolecular triads and charge separation within the triads.

Acknowledgment. The authors are thankful to the donors of the Petroleum Research Fund, administered by the American Chemical Society and National Institutes of Health (to F.D.) for support of this work.

Supporting Information Available: Absorption spectrum of **2**, **4**, and ZnP in *o*-dicholorobenzene. This material is available free of charge via the Internet at http://pubs.acs.org.

References and Notes

(1) (a) Maruyama, K.; Osuka, A. *Pure Appl. Chem*. **1990**, *62*, 1511. (b) Gust, D.; Moore, T. A. *Science* **1989**, *244*, 35. (c) Gust, D.; Moore, T. A. *Top. Curr. Chem*. **1991**, *159*, 103. (d) Gust, D.; Moore, T. A.; Moore, A. L. *Acc. Chem. Res*. **1993**, *26*, 198. (e) Wasielewski, M. R. *Chem. Rev*. **1992**, *92*, 435. (f) Paddon-Row: M. N. *Acc. Chem. Res*. **1994**, *27*, 18. (g) Sutin, N. *Acc. Chem. Res*. **1983**, *15*, 275. (h) Bard, A. J.; Fox, M. A. *Acc. Chem. Res*. **1995**, *28*, 141. (i) Meyer, T. J. *Acc. Chem. Res.* **1989**, *22*, 163. (j) Piotrowiak, P. *Chem. Soc. Rev*. **1999**, *28*, 143.

(2) (a) Ward, M. W. *Chem. Soc. Rev*. **1997**, *26*, 365 and references therein. (b) Hayashi, T.; Ogoshi, H. *Chem. Soc. Rev*. **1997**, *26*, 355. (c) Sessler, J. S.; Wang, B.; Springs, S. L.; Brown, C. T. In *Comprehensive Supramolecular Chemistry*; Atwood, J. L., Davies, J. E. D., MacNicol, D. D., Vögtle, F., Eds.; Pergamon: Oxford, U.K., 1996; Chapter 9. (d) Feldheim D. L.; Keating, C. D. *Chem. Soc. Rev*. **1998**, *27*, 1. (e) *Introduction of Molecular Electronics*; Petty, M. C., Bryce, M. R., Bloor, D., Eds.; Oxford University Press: New York, 1995. (f) Emmelius, M.; Pawlowski, G.; Vollmann, H. W *Angew. Chem., Int. Ed. Engl*. **1989**, *28*, 1445.

(3) (a) Diesenhofer, J.; Michel, H. *Angew. Chem., Int. Ed. Engl*. **1989**, *28*, 829. (b) Feher, J. P.; Allen, M. Y.; Okamura, M. Y.; Rees, D. C. *Nature* **1989**, *339*, 111.

(4) (a) Connolly, J. S.; Bolton, J. R. In *Photoinduced Electron Transfer*; Fox, M. A., Channon, M., Eds.; Elsevier: Amsterdam, 1988; Part D, pp 303−393. (b) Antolovich, M.; Keyte, P. J.; Oliver, A. M.; Paddon-Row, M. N.; Droon, J.; Verhoever, J. W.; Jonker, S. A.; Warman, J. M. *J. Phys. Chem*. **1991**, *95*, 1933. (c) Macpherson, A. N.; Liddell, P. A.; Lin, S.; Noss, L.; Seely, G. R.; DeGraziano, J. M.; Moore, A. L.; Moore, T. A.; Gust, D. *J. Am. Chem. Soc*. **1995**, *117*, 7202.

(5) (a) Kroto, H. W.; Heath, J. R.; O'Brien, S. C.; Curl, R. F.; Smalley, R. E. *Nature* **1985**, *318*, 162. (b) Kratschmer, W.; Lamb, L. D.; Fostiropoulos F.; Huffman, D. R. *Nature* **1990**, *347*, 345.

(6) *Fullerene and Related Structures*; Hirsch, A., Ed.; Springer: Berlin, 1999; Vol. 199.

(7) (a) Allemand, P. M.; Koch, A.; Wudl, F.; Rubin, Y.; Diederich, F.; Alvarez, M. M.; Anz S. J.; Whetten, R. L. *J. Am. Chem. Soc*. **1991**, *113*, 1050. (b) Xie, Q.; Perez-Cordero, E.; Echegoyen, L. *J. Am. Chem. Soc*. **1992**, *114*, 3978.

(8) Ajie, H.; Alvarez, M. M.; Anz, S. J.; Beck, R. E.; Diederich, F.; Fostiropoulos, K.; Huffman, D. R.; Kratschmer, W.; Rubin, Y.; Schriver, K. E.; Sensharma E.; Whetten, R. L. *J. Phys. Chem*. **1990**, *94*, 8630.

(9) Imahori, H.; Hagiwara, K.; Akiyama, T.; Aoki, Ml; Taniguchi, S.; Okada, T.; Shirakawa, M.; Sakata, Y. *Chem. Phys. Lett*. **1996**, *263*, 545.

(10) (a) Khan, S. I.; Oliver, A. M.; Paddon-Row: M. N.; Rubin, Y. *J. Am. Chem. Soc*. **1993**, *115*, 4919. (b) Saricciftci, N. S.; Wudl, F.; Heeger, A. J.; Maggini, M.; Scorrano, G.; Prato, M.; Bourassa, J.; Ford, P. C. *Chem. Phys. Letts*. **1995**, *247*, 510. (c) Liddell, P. A.; Sumia, J. P.; Macpherson, A. N.; Noss, L.; Seely, G. R.; Clark, K. N.; Moore, A. L.; Moore T. A.; Gust, D. *Photochem. Photobiol*. **1994**, *60*, 537. (d) Williams, R. M.; Zwier, J. M.; Verhoever, J. W. *J. Am. Chem. Soc*. **1995**, *117*, 4093. (e) Imahori, H.; Hagiwara, K.; Aoki, M.; Akiyama, T.; Taniguchi, S.; Okada, T.; Shirakawa, M.; Sakata, Y. *J. Am. Chem. Soc*. **1996**, *118*, 11771. (f) Kuciauskas, D.; Lin, S.; Seely, G. R.; Moore, A. L.; Moore, T. A.; Gust, D.; Drovetskaya, T.; Reed, C. A.; Boyd, P. D. W. *J. Phys. Chem*. **1996**, *100*, 15926. (g) Guldi, D. M.; Maggini, M.; Scorrano, G.; Prato, M. *J. Am. Chem. Soc*. **1997**, *119*, 974. (h) Imahori, H.; Yamada, K.; Hasegawa, M.; Taniguchi, S.; Okada, T.; Sakata, Y. *Angew. Chem., Int. Ed. Engl*. **1997**, *36*, 2626. (h) Liddell, P. A.; Kuciauska, D.; Sumida, J. P.; Nash, B.; Nguyen, D.; Moore, A. L.; Moore, T. A.; Gust, D. *J. Am. Chem. Soc*. **1997**, *119*, 1400.

(11) (a) Dietel, E.; Hirsh, A.; Eichhorn, E.; Rieker, A.; Hackbarth, S.; Roder, B. *Chem. Commun*. **1998**, 1981. (b) Gareis, T.; Kothe, O.; Daub, J. *Eur. J. Org. Chem*. **1998**, 1549. (c) Da Ros, T.; Prato, M.; Guldi, D.; Alessio, E.; Ruzzi, M.; Pasimeni, L.; Carano, M.; Paolucci, F.; Ceroni, P.; Roffia, S. In *Recent Advances in the Chemistry and Physics of Fullerenes and Related Materials*; Kadish, K. M., Ruoff, R. S., Eds.; The Electrochemical Proceedings Series; Electrochemical Society: Pennington, NJ, 1998; p 1074. (d) Martin, N.; Sanchez, L.; Illescas, B.; Perez, I. *Chem. Rev*. **1998**, *98*, 2527. (e) Gareis, T.; Kothe, O.; Daub, J. *Eur. J. Org. Chem*. **1998**, 1549.

(12) (a) Guldi, D. M. *Chem. Commun*. **2000**, 321. (b) Armaroli, N.; Marconi, G.; Echegoyen, L.; Bourgeois, J.-P.; Diederich, F. *Chem. Eur. J*. **2000**, *6*, 1629. (c) Guldi, D. M.; Luo, C.; Da Ros, T.; Prato, M.; Dietel, E.; Hirsch, A. *Chem. Commun*. **2000**, 375. (d) Luo, C.; Guldi, D. M.; Imahori, H.; Tamaki, K.; Sakata, Y. *J. Am. Chem. Soc*. **2000**, *122*, 6535. (e) Kuciauskas, D.; Liddell, P. A.; Lin, S.; Stone, S. G.; Moore, A. L.; Moore, T. A.; Gust, D. *J. Phys. Chem. B* **2000**, *104*, 4307. (f) Schuster, D. I.; Cheng, P.; Wilson, S. R.; Prokhorenko, V.; Katterie, M.; Holzwarth, A. R.; Braslavsky, S. E.; Klihm, G.; Williams, R. M. Luo, C. *J. Am. Chem. Soc*. **2000**, *121*, 11599. (g) Tashiro, K.; Aida, T.; Zheng, J.-Y.; Kinbara, K.; Saigo, K.; Sakamoto, S.; Yamaguchi, K. *J. Am. Chem. Soc*. **1999**, *121*, 9477. (h) Tkachenko, N. V.; Rantala, L.; Tauber, A. Y.; Helaja, J.; Hynninen, P. H.; Lemmetyinen, H. *J. Am. Chem. Soc*. **1999**, *121*, 9378. (i) D'Souza, F.; Zandler, M. E.; Smith, P. M.; Deviprasad, G. R.; Arkady, K.; Fujitsuka, M.; Ito, O. *J. Phys. Chem. A* **2002**, *106*, 649.

(13) (a) D'Souza, F.; Deviprasad, G. R.; Rahman, M. S.; Choi, J.-P. *Inorg. Chem*. **1999**, *38*, 2157. (b) Armaroli, N.; Diederich, F.; Echegoyen, L.; Habicher, T.; Flamigni, L.; Marconi, G.; Nierengarten, J.-F. *New J. Chem*. **1999**, 77. (c) Da Ros, T.; Prato, M.; Guldi, D. M.; Alessio, E.; Ruzzi, M.; Pasimeni, L. *Chem. Commun*. **1999**, 635. (d) Deviprasad, G. R.; Zandler, M. E.; D'Souza, F. In *Fullerenes 2000: Electrochemistry and Photochemistry*; Fukuzumi, S., D'Souza, F., Guldi, D. M., Eds.; Proceedings of the Electrochemical Society; Electrochemical Society: Pennington, NJ, 2000; No. 8, p 182. (e) D'Souza, F.; Rath, N. P.; Deviprasad, G. R.; Zandler, M. E. *Chem. Commun*. **2001**, 267. (f) Da Ros, T.; Prato, M.; Guldi, D. M.; Ruzzi, M.; Pasimeni, L. *Chem. Eur. J*. **2001**, *7*, 816.

(14) D'Souza, F.; Deviprasad, G. R.; El-Khouly, M. E.; Fujitsuka, M.; Ito, O. *J. Am. Chem. Soc*. **2001**, *123*, 5277.

(15) Frisch, M. J.; Trucks, G. W.; Schlegel, H. B.; Scuseria, G. E.; Robb, M. A.; Cheeseman, J. R.; Zakrzewski, V. G.; Montgomery, J. A.; Stratmann, R. E.; Burant, J. C.; Dapprich, S.; Millam, J. M.; Daniels, A. D.; Kudin, K. N.; Strain, M. C.; Farkas, O.; Tomasi, J.; Barone, V.; Cossi, M.; Cammi, R.; Mennucci, B.; Pomelli, C.; Adamo, C.; Clifford, S.; Ochterski, J.; Petersson, G. A.; Ayala, P. Y.; Cui, Q.; Morokuma, K.; Malick, D. K.; Rabuck, A. D.; Raghavachari, K.; Foresman, J. B.; Cioslowski, J.; Ortiz, J. V.; Stefanov, B. B.; Liu, G.; Liashenko, A.; Piskorz, P.; Komaromi, I.; Gomperts, R.; Martin, R. L.; Fox, D. J.; Keith, T.; Al-Laham, M. A.; Peng, C. Y.; Nanayakkara, A.; Gonzalez, C.; Challacombe, M.; Gill, P. M. W.; Johnson, B. G.; Chen, W.; Wong, M. W.; Andres, J. L.; Head-Gordon, M.; Replogle, E. S.; Pople, J. A. *Gaussian 98*, Revision A.7; Gaussian, Inc.: Pittsburgh, PA, 1998.

(16) (a) Matsumoto, K.; Fujitsuka, M.; Sato, T.; Onodera, S.; Ito, O. *J. Phys. Chem. B* **2000**, *104*, 11632. (b) Komamine, S.; Fujitsuka, M.; Ito, O.; Morikawa, K.; Miyata, T.; Ohno, T. *J. Phys. Chem. A* **2000**, *104*, 11497.

(17) D'Souza, F.; Hsieh, Y.-Y.; Deviprasad, G. R. *Inorg. Chem*. **1996**, *35*, 5747.

(18) Kadish, K. M.; Van Caemelbecke, E.; Royal, G. In *The Porphyrin Handbook*; Kadish, K. M., Smith, K. M., Guilard, R., Eds.; Academic Press: New York, 2000; Vol. 55, Chapter 1.

(19) Echegoyen, L.; Echegoyen, L. E. *Acc. Chem. Res*. **1998**, *31*, 593.

(20) Bonnett, R.; McGarvey, D. J.; Harriman, A.; Land, E. J.; Truscott, T. G.; Winfield, U.-J. *Photochem. Photobiol*. **1988**, *48*, 271.

(21) (a) Seybold, P. G.; Gouterman, M. *J. Mol. Spectros*. **1969**, *31*, 1. (b) Quimby, D. J.; Longo, F. R. *J. Am. Chem. Soc*. **1975**, *97*, 5111.

(22) The room-temperature binding constants (*K*) for 2-(3′ or 4′-pyridyl)-fulleroopyrrolidine and ZnP in *o*-dichlorobenzene are about $7.6 \times 10^3\ M^{-1}$ (ref 13a,d). Attempts to obtain the binding constants for the equilibrium reactions involving **1** or **2** and ZnP by optical absorption or ^1H NMR

spectroscopic methods were unsuccessful because of the strong absorption and/or overlapping ^{1}H resonance peaks of added porphyrins. However, on the basis of the previously reported *K* values for 2-(3′ or 4′-pyridyl)-fulleropyrrolidine binding to ZnP (ref 13a,d), and by neglecting any steric effects caused by the covalently linked by flexible bonds free-base porphyrin, a *K* value of about 7.6×10^3 M^{-1} is assumed for the equilibrium reactions involving **1** or **2** and ZnP.

(23) Imahori, H.; El-Khouly, M. E.; Fujitsuka, M.; Ito, O.; Sakata, Y.; Fukuzumi, S. *J. Phys. Chem. A* **2001**, *105*, 325.

(24) Nojiri, T.; Watanabe, A.; Ito, O. *J. Phys. Chem. A* **1998**, *102*, 5215.

(25) (a) Ghosh, H. N.; Pal, H.; Sapre, A. V.; Mittal, J. P. *J. Am. Chem. Soc.* **1993**, *115*, 11722. (b) Fujitsuka, M.; Ito, O.; Yamashiro, T.; Aso, Y.; Otsubo, T. *J. Phys. Chem. A* **2000**, *104*, 4876.

(26) El-Khouly, M. E.; Fujitsuka, M.; Ito, O. *J. Porphyrins Phthalocyanines* **2000**, *4*, 590.

(27) In *o*-dichlorobenzene, decay rate of ^{3}ZnP* (at 850 nm) is as fast as that in benzonitrile, although the formation of $C_{60}^{\bullet-}$ in *o*-dichlorobenzene is smaller than that in benzonitrile (ref 26).

(28) Imahori, H.; Tamaki, K.; Guldi, D. M.; Luo, C.; Fujitsuka, M.; Ito, O.; Sakata, Y.; Fukuzumi, S. *J. Am. Chem. Soc.* **2001**, *123*, 2607.